PDFS DETERMINATION FROM THE LHeC*

Francesco Giuli

on behalf of the LHeC/FCC-eh study groups

CERN, EP Department, 1211 Geneva 23, Switzerland
francesco.giuli@cern.ch

Received 12 February 2023, accepted 30 March 2023, published online 6 September 2023

Deep Inelastic Scattering would be brought into the unexplored TeV regime by the proposed Large Hadron Electron Collider at CERN. Its rich physics program includes both precision Standard Model measurements to complement LHC physics as well as studies of QCD in the high-energy limit. The present contribution reports on studies included in the updated LHeC Conceptual Design Report. We study the impact of LHeC simulated data on Parton Distribution Functions uncertainties. We also assess the LHeC potential to allow for the determination of the strong coupling constant α_S, at the per-mille level as well as to disentangle between various scenarios of small-x QCD.

DOI:10.5506/APhysPolBSupp.16.7-A22

1. The Large Hadron Electron Collider

The Conceptual Design Report (CDR) of the Large Hadron Electron Collider (LHeC) was published in 2012 [1]. The advantage of an *ep* collider is that it offers the opportunity to observe phenomena which would be observed in a *pp* collider with a cleaner decay environment. The LHeC would provide a 60 GeV energy electron beam which would be collided with hadron beams already from the LHC. In this way, there would be an increase of two orders of magnitude over the integrated HERA luminosity, and the kinematic range would be increased by a factor of ~ 25 for Q^2 and $1/x$.

The LHeC experiment could be realized in the 2030s during the High-Luminosity LHC (HL-LHC) and it will provide an unprecedented resolution of the partonic constituents in hadronic matter up to $x \sim 0.9$ and down to Bjorken $x \sim 10^{-6}$.

* Presented at the 29$^{\text{th}}$ Cracow Epiphany Conference on *Physics at the Electron–Ion Collider and Future Facilities*, Cracow, Poland, 16–19 January, 2023.

2. Simulated samples

In order to estimate the impact of LHeC data on the uncertainties of Parton Distribution Functions (PDFs), several sets of LHeC inclusive Neutral-Current and Charged-Current Deep Inelastic Scattering (NC and CC DIS) data have been simulated, with a full set of systematic uncertainties. The largest source of uncertainties is due to the hadronic energy scale, global efficiency uncertainty, and photo-production background. An improvement by at most a factor of two with respect to H1's achievements is foreseen.

The bulk of the data is assumed to be taken with electrons, characterized by large negative helicity P_e. It is assumed there will be an initial phase during which the LHeC may collect 50 fb^{-1} of data (first three years), while the total luminosity is assumed to be close to 1 ab^{-1}, a very high value when compared with HERA.

3. PDFs determination

The expected sensitivity of LHeC data on PDFs determinations was presented in Ref. [2]. Fits in NNLO QCD have been performed to the above-described simulated data. The HERAPDF procedure [3] has been followed closely, and the following parametric functions have been adopted. The quark distributions at the initial scale $Q_0^2 = 1.9$ GeV^2 are parametrised by

$$xq_i(x) = A_i x^{B_i}(1-x)^{C_i} P_i(x)\,, \tag{1}$$

where $P_i(x) = (1 + D_i x + E_i x^2)$ and the flavour of the quark distribution is specified by the index i. The A_{u_V} and A_{d_V} parameters are fixed using the quark counting rule, while the normalisation and the slope of the $\bar{u}$ and $\bar{d}$ distributions are set equal for $x \to 0$. The strange quark PDF, $x\bar{s}$, is set to be a fraction of the $x\bar{d}$ distributions, namely $x\bar{s} = r_s x\bar{d}$ with $r_s = 0.67$.

The gluon PDF, xg, uses a different parametrisation

$$xg(x) = A_g x^{B_g}(1-x)^{C_g} - A_g^{'} x^{B_g^{'}}(1-x)^{C_g^{'}}\,. \tag{2}$$

The momentum sum rule fixes A_g, the normalisation parameter, while $C_g^{'}$ is set to 25 to suppress negative contributions at high x.

The parametrised PDFs at the starting scale Q_0^2 are the valence distributions, xu_V and xd_V, the gluon distribution, xg, and the sea distributions $x\bar{U}$ and $x\bar{D}$, being $x\bar{U} = x\bar{u}$ and $x\bar{D} = x\bar{d} + x\bar{s}$. The nominal fits have 14 free parameters, which are similar to HERAPDF2.0, albeit more flexible due to the stronger constraints from the LHeC.

3.1. Valence distributions

Figure 1 illustrates the precision that can be expected for the valence quark distributions, where it is compared to a selection of modern PDF sets,

namely ABMP16 [4], NNPDF4.0 [5], CT18 [6], MSHT20 [7], HERAPDF2.0 [3], and PDF4LHC21 [8]. While the improvement in the determination of the u_V distribution is not substantial, a striking advance in d_V is visible when adding the LHeC data. In particular, the strong constraints to the very high-x regime are due to the high integrated luminosity. Note that the yellow band, which displays the "LHeC 1st run" PDF, includes only electron and no positron data. Indeed, differences access to valence quarks at low-x can be obtained from the $e^{\pm}p$ cross section.

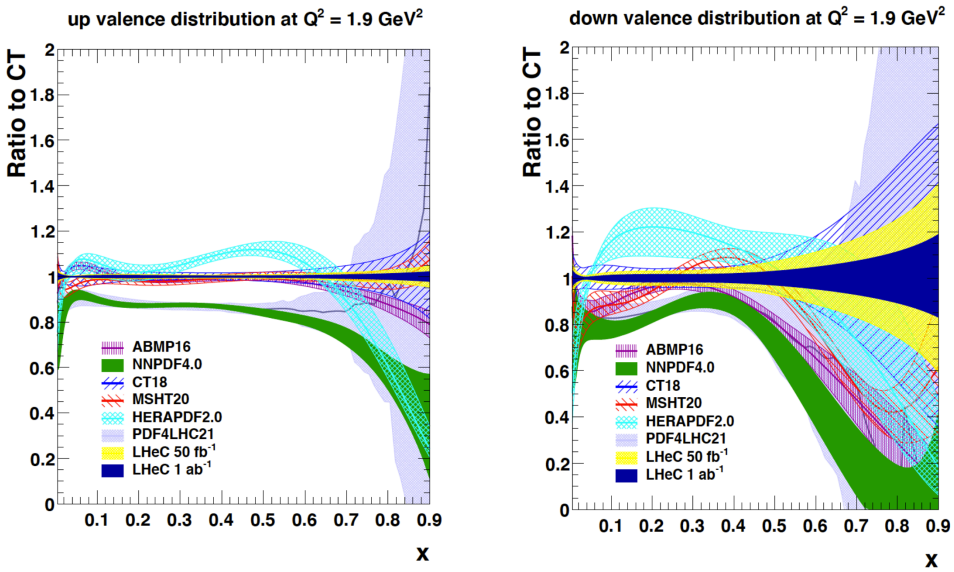


Fig. 1. (Colour on-line) Valence quark distributions at $Q^2 = 1.9$ GeV^2 as a function of x, displayed as a ratio to the CT18 [6] PDF set. The yellow band corresponds to the "LHeC 1st run" PDFs, while the dark blue one shows the final "LHeC inclusive" PDFs based on the full LHeC data sets. For the purposes of illustrating the improvement to the uncertainties more clearly, the central values of the LHeC PDFs have been scaled to the CT18 PDF, which itself is displayed by the green band. These plots are taken from Ref. [2].

The precise determination of the u_V and d_V PDFs in the high-x regime is particularly relevant for Beyond the Standard Model (BSM) searches. A precise determination of the valence quarks distributions will allow for the discrimination about current conflicting theoretical pictures for the d_V/u_V ratio, which cannot be determined precisely with present data, which are inconclusive statistically and suffer from large uncertainties from the use of DIS data on nuclear targets.

3.2. Anti-quarks distributions

With LHeC data, our knowledge about the sea-quark PDFs will be changed completely. The $x\bar{U}$ and $x\bar{D}$ PDFs from the 1st run and the "LHeC inclusive" are shown in Fig. 2 for $Q^2 = 1.9$ GeV^2. A remarkable increase in the determination of the $x\bar{U}$ and $x\bar{D}$ distributions is visible and it persists from low- to high-x.

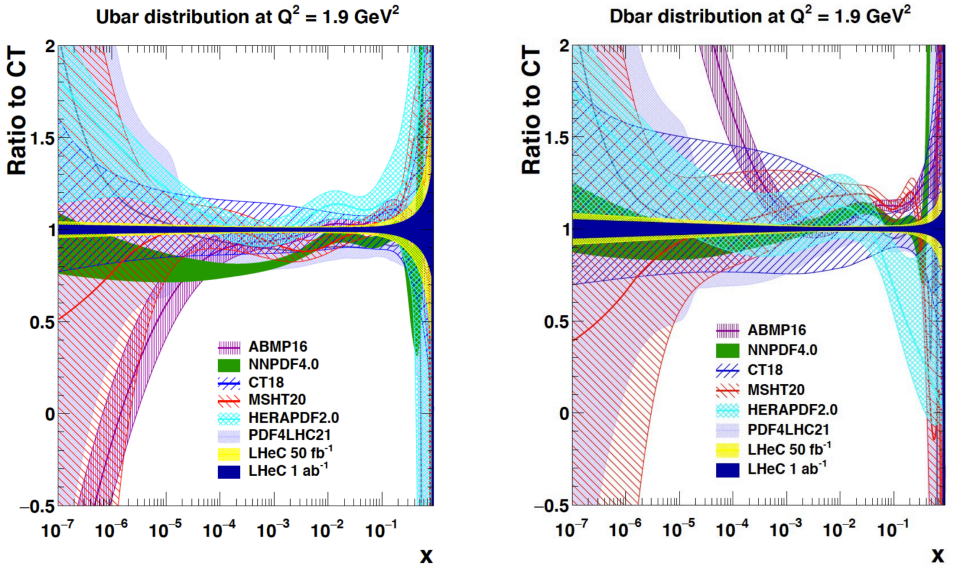


Fig. 2. (Colour on-line) Anti-quark distributions at $Q^2 = 1.9$ GeV^2 as a function of x, displayed as a ratio to the CT18 [6] PDF set. The yellow band corresponds to the "LHeC 1st run" PDFs, while the dark blue one shows the final "LHeC inclusive" PDFs based on the full LHeC data sets. For the purposes of illustrating the improvement to the uncertainties more clearly, the central values of the LHeC PDFs have been scaled to the CT18 PDF, which itself is displayed by the green band. These plots are taken from Ref. [2].

However, the relative uncertainties for $x \geq 0.5$ are large. This is not particularly worrisome, since the sea-quark contributions are already very tiny in that region. The value of the full LHeC data sample is recognisable in the high-x regime, while the uncertainties of both the small and the full data sets are comparable (and very small) for $x \lesssim 0.1$.

3.3. The gluon distribution

With an extended kinematic range of DIS and hugely increased precision, the LHeC data can advance our knowledge of the gluon PDF, xg, and pin it down much more accurately than it is currently known.

Figure 3 shows the gluon distribution, as it is obtained from the fit to the LHeC inclusive NC and CC data. When including the LHeC NC and CC precision data, the determination of the gluon PDF will improve dramatically, from the very low-x values, $\geq 10^{-5}$, to large $x \leq 0.8$. It is visible how a precision of a few percent is achieved down to $x \sim 10^{-5}$ and this will help in resolving the question of non-linear parton interactions at small-x.

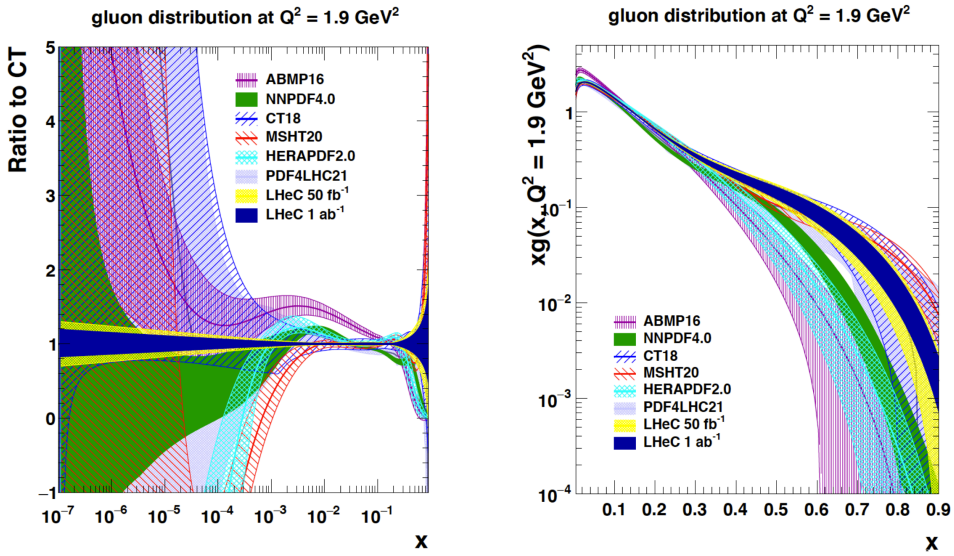


Fig. 3. (Colour on-line) Gluon distribution at $Q^2 = 1.9$ GeV^2 as a function of x, displayed as a ratio to the CT18 [6] PDF set. The yellow band corresponds to the "LHeC 1$^{\text{st}}$ run" PDFs, while the dark blue one shows the final "LHeC inclusive" PDFs based on the full LHeC data sets. For the purposes of illustrating the improvement to the uncertainties more clearly, the central values of the LHeC PDFs have been scaled to the CT18 PDF, which itself is displayed by the green band. Left: the distribution is shown on a logarithm x scale and highlights the low-x region. Right: the distribution is shown on a linear x scale and highlights the high-x region. These plots are taken from Ref. [2].

Furthermore, in the large-x region, $x \gtrsim 0.3$, the very large luminosity provides NC and CC data to accurately access the highest values of x, disentangling the sea from the dominant valence part. Thanks to the seminal coverage from very small values of x up to $x \sim 1$, the gluon PDF can be largely constrained through the momentum sum-rule, and the resulting small uncertainties in the high-x regime are of great importance from BSM searched in pp collisions.

3.4. Parton luminosities

It is extremely convenient to express the usefulness of the PDF determinations performed at the LHeC with the so-called "parton luminosities". These are defined as follows:

$$L_{ab}(M_X) = \int \mathrm{d}x_a \mathrm{d}x_b \sum_q F_{ab} \delta\left(M_X^2 - s x_a x_b\right), \tag{3}$$

where F_{ab} for $(a,b) = (q\bar{q})$ is defined as

$$F_{q\bar{q}} = x_1 x_2 \left[q\left(x_1, M^2\right) \bar{q}\left(x_2, M^2\right) + \bar{q}\left(x_1, M^2\right) q\left(x_2, M^2\right)\right], \tag{4}$$

and (a,b) could also be (g,q), $(g,\bar{q})$, and (gg), without a sum over quarks in the latter case. Figure 4 illustrates the expectations for the quarks and gluon parton luminosities. Very precise predictions in a vast range of M_X can be provided by the LHeC. This basically eliminates the main sources of uncertainties due to currently sizeable PDF errors in precision electroweak

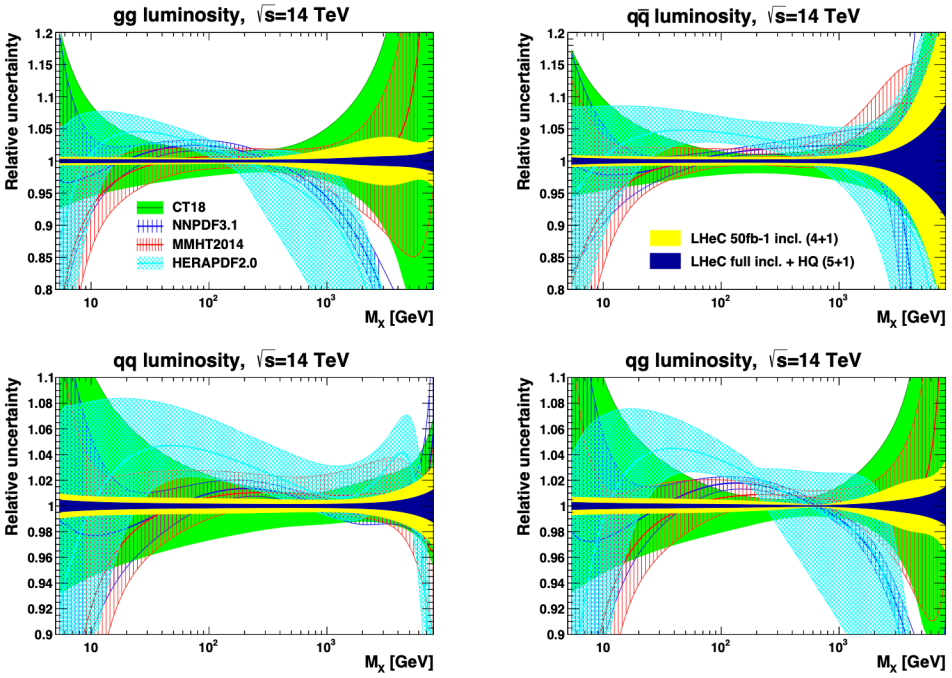


Fig. 4. (Colour on-line) Uncertainty bands for parton luminosities as a function of the mass $M_X = \sqrt{s x_1 x_2}$ for LHC energies. The yellow band corresponds to the "LHeC 1st run" PDFs, while the dark blue one shows a fit to the LHeC inclusive data sets. Both LHeC PDFs shown are scaled to the central value of the CT18 PDF set [6]. These plots are taken from Ref. [2].

(EW) measurements performed at the LHC (*i.e.* the determination of the W boson mass, m_W, to be within 10^{-4} uncertainty). Moreover, the gluon–gluon luminosity can be determined at 1%-level for the Higgs mass $M_X = M_H \backsimeq 125$ GeV, a factor two or three better than current determinations.

4. Precise determination of the strong coupling constant

Since jet cross sections are proportional to $\mathcal{O}(\alpha_S)$ already at leading-order (LO) QCD, the measurement of these production cross sections at the LHeC will provide sensitivity to the strong coupling constant $\alpha_S(m_Z)$ [9]. Jets with transverse momentum, p_T, between 3 and 500 GeV will be recorded at the LHeC, where the jet energy scale can be calibrated with very high accuracy. It can reach an uncertainty significantly smaller than present LHC experiments, ranging from 0.3% up to 0.5%. This can be directly translated into an overall uncertainty of about 5% (at the very most) on the jet cross section in the Breit frame [2].

Performing simultaneous extractions of PDFs+α_S when fitting inclusive DIS and jet data together, an uncertainty of $\delta\alpha_S(m_Z) = \pm\ 0.00018$ [2] can be achieved. This value is smaller than the present world average by more than a factor of five, and it will be a challenge to have equally accurate theoretical predictions at N^{3}LO or even beyond.

Other related measurements of the hadronic final states, such as multi-jet cross sections, jet substructure observables, n-jettiness observables, or event shapes could be included in future PDF fits, and commonly enlarge the sensitivity to the gluon PDF. Moreover, further sensitivity to Transverse Momentum Dependent (TMD) effects can be achieved analysing precision measurements of lepton–jet decorrelation observables [10, 11].

5. Investigating new small- and high-x dynamics

Due to the high ep center-of-mass energy, the large acceptance of the LHeC detector and the expected high luminosity of the accelerators, the physics in the low-x regime can be accurately studied at the LHeC. In contrast to LHC pp data, since only a single hadron is involved in the collisions happening at the LHeC, the PDF determinations are free from low-x–high-x correlations, and the physics phenomena in these two extreme regions can be studied separately with high precision.

In the large-x region, the higher twists effects become negligible thanks to the ample statistics at such a high Q^2. This is particularly relevant for constraining BSM signatures with large mass scales.

At small-x, the sea quark and the gluon densities rise so much that non-linear and possibly saturation effects may become manifest, as already observed at HERA. These novel dynamics can be studied in ep and eA collisions at the LHeC for the first time in a reliable way, given that the strong coupling constant is small at such high scales. This might replace the DGLAP evolution by non-linear evolution and/or BFKL-type equations, with major consequences for physics measurements performed at future hadron colliders (HL-LHC and beyond) [12, 13]. With new measurements of diffractive DIS cross sections, the field of diffractive PDFs will gain new interest [14].

6. Conclusion

Undoubtedly, our present knowledge of the proton structure has been driven by measurements performed at HERA. With its 1000 times larger luminosity (and higher kinematic reach, as well as center-of-mass energy), the LHeC will equally provide relevant experimental data for precision PDF physics. Furthermore, such independent PDFs are of crucial importance to achieve the physics goal of the HL-LHC programme. Moreover, it has been shown how the large luminosity of the LHeC provides high experimental precision at high x, allowing a determination of the strong coupling constant α_S at 0.1%-level. Furthermore, non-linear and possibly saturation effects can be nicely studied in the low-x region.

REFERENCES

[1] LHeC Study Group (J.L. Abelleira Fernandez *et al.*), *J. Phys. G: Nucl. Part. Phys.* **39**, 075001 (2012), arXiv:1206.2913 [physics.acc-ph].

[2] LHeC and FCC-he Study Group (P. Agostini *et al.*), *J. Phys. G: Nucl. Part. Phys.* **48**, 110501 (2021), arXiv:2007.14491 [hep-ex].

[3] H1 and ZEUS collaborations (H. Abramowicz *et al.*), *Eur. Phys. J. C* **75**, 580 (2015), arXiv:1506.06042 [hep-ex].

[4] S. Alekhin *et al.*, *Phys. Rev. D* **96**, 014011 (2017), arXiv:1701.05838 [hep-ph].

[5] NNPDF Collaboration (R.D. Ball *et al.*), *Eur. Phys. J. C* **82**, 428 (2022), arXiv:2109.02653 [hep-ph].

[6] T.J. Hou *et al.*, *Phys. Rev. D* **103**, 014013 (2021), arXiv:1912.10053 [hep-ph].

[7] S. Bailey *et al.*, *Eur. Phys. J. C* **81**, 341 (2021), arXiv:2012.04684 [hep-ph].

[8] PDF4LHC Working Group (R.D. Ball *et al.*), *J. Phys. G: Nucl. Part. Phys.* **49**, 080501 (2022), arXiv:2203.05506 [hep-ph].

[9] H1 Collaboration (V. Andreev *et al.*), *Eur. Phys. J. C* **77**, 791 (2017), *Erratum ibid.* **81**, 738 (2021), arXiv:1709.07251 [hep-ex].

[10] X. Liu *et al.*, *Phys. Rev. Lett.* **122**, 192003 (2019), arXiv:1812.08077 [hep-ph].

[11] H1 Collaboration (V. Andreev *et al.*), *Phys. Rev. Lett.* **128**, 132002 (2022), arXiv:2108.12376 [hep-ex].

[12] M. Bonvini, S. Marzani, *Phys. Rev. Lett.* **120**, 202003 (2018), arXiv:1802.07758 [hep-ph].

[13] M. Bonvini, *Eur. Phys. J. C* **78**, 834 (2018), arXiv:1805.08785 [hep-ph].

[14] N. Armesto *et al.*, *Phys. Rev. D* **100**, 074022 (2019), arXiv:1901.09076 [hep-ph].